AJNR

MR Imaging of Cavernous Sinus Involvement by Pituitary Adenomas

Giuseppe Scotti, Chin-Yin Yu, William P. Dillon, David Norman, Nadia Colombo, Thomas H. Newton, Jack De Groot and Charles B. Wilson

AJNR Am J Neuroradiol 1988, 9 (4) 657-664
http://www.ajnr.org/content/9/4/657

MR Imaging of Cavernous Sinus Involvement by Pituitary Adenomas

Giuseppe Scotti[1, 2]
Chin-Yin Yu[1, 3]
William P. Dillon[1]
David Norman[1]
Nadia Colombo[1, 4]
Thomas H. Newton[1]
Jack De Groot[5]
Charles B. Wilson[6]

The ability of high-resolution MR imaging (1.5 T) to detect invasion of the cavernous sinuses by pituitary adenoma was determined through a retrospective review of 74 patients. These patients were divided into three groups: 25 normal subjects, 24 subjects with invasive pituitary adenomas, and 25 subjects with noninvasive pituitary adenomas. A fourth group of 30 patients, who subsequently underwent surgery for pituitary adenoma, was evaluated prospectively by MR for the presence or absence of cavernous sinus invasion. Several features were analyzed: (1) the detectability of the medial and lateral dural margins of the cavernous sinus (2) the size and variation in intensity of compartments within the cavernous sinus (3) the relationship of endocrine function to the surgical and MR appearance of the cavernous sinus and (4) carotid artery displacement or encasement by tumor. The normal cavernous sinuses were usually symmetric, but their sizes varied. The lateral dural margin of the cavernous sinus was always recognized on MR as a linear, discrete, low-intensity area. The medial dural margin (pituitary capsule) was seen on MR in only two of the 25 normal patients. In all 24 patients with cavernous sinus invasion involvement was unilateral and was most common with laterally positioned prolactin or adrenocorticotropic hormone secretory adenomas. Invasion of the cavernous sinus was suspected by MR in only two of the 13 invasive microadenomas and was questionable in three. In 10 of the 11 macroadenomas with surgically proved dural invasion, MR demonstrated an asymmetric increase in size and intensity of the superior and inferior cavernous sinus compartments. Noninvasive macroadenomas compressed and displaced the cavernous sinus bilaterally.

The prospective MR evaluation of 30 patients undergoing surgery for pituitary tumor revealed a sensitivity for predicting cavernous sinus invasion of 55%, a specificity of 85.7%, a positive predictive value of 62.5%, and a negative predictive value of 81.8%. No feature permitted certain distinction between invasive and noninvasive microadenomas, as the medial dural wall of the cavernous sinus could not be reliably identified. The most specific sign of cavernous sinus invasion was carotid artery encasement.

This article appears in the July/August 1988 issue of *AJNR* and the October 1988 issue of *AJR*.

Received August 10, 1987; accepted after revision December 31, 1987.

[1] Department of Radiology (L-358), Diagnostic and Interventional Neuroradiology Section, University of California, San Francisco, CA 94143. Address reprint requests to W. P. Dillon.

[2] Istituto di Science Radiologiche, Cattedra di Neuroradiologia, University of Milan, Italy.

[3] Department of Diagnostic Radiology, Cheng-Kung University, Tainan, Taiwan.

[4] Servizio di Neuroradiologia, Ospedale Niquarda Ca Granda, Milan, Italy.

[5] Department of Anatomy, University of California, San Francisco, CA 94143.

[6] Department of Neurosurgery, University of California, San Francisco, CA 94143.

***AJNR* 9:657–664, July/August 1988**
0195–6108/88/0904–0657

Pituitary adenomas frequently involve the cavernous sinuses. The extent of involvement may include (1) displacement and compression of the medial walls of the cavernous sinus, (2) microscopic infiltration of the dura of the medial wall [1, 2], or (3) extensive invasion of the sinus with or without encasement of the carotid artery [3–5].

Cavernous sinus invasion (CSI) by pituitary tumors is found more often at surgery than has been previously appreciated [2, 6–8]. Adenomas that involve the cavernous sinus are characterized as invasive or aggressive [4, 5]. Although no features of malignancy are usually found on histologic examination, these aggressive adenomas have a less favorable prognosis, probably because complete removal of the tumor is less likely [9]. The prognosis, surgical morbidity, and therapeutic treatment planning for pituitary tumors might be improved if preoperative determination of the presence and extent of cavernous sinus involvement was possible. Reports in the literature suggest that CT is a reliable means of demonstrating the normal and abnormal anatomy of the cavernous sinus [10–12] and CSI by pituitary tumors [12]. Although high-field, high-resolution MR has proved to be superior to

both lower field MR and CT in imaging the normal and abnormal pituitary gland and sellar region [13–16], only a few anecdotal cases of CSI by a pituitary adenoma have been reported with the use of MR imaging [12].

The purpose of our study was to review the normal MR anatomy of the cavernous sinus and to determine the ability of this imaging method to provide reliable information and definitive proof of the presence or absence of CSI by pituitary adenomas.

Materials, Subjects, and Methods

Our study comprised a retrospective review of the MR scans of 74 patients and a prospective analysis of 30 patients with pituitary adenomas.

Retrospective Analysis

In the retrospective phase of this study, the MR examinations of the sellar region of 74 patients were reviewed. These patients were divided into three groups: (1) 25 normal subjects (six male and 19 female) 13–66 years old (mean, 38 years) with normal pituitary glands and no known endocrinologic or cavernous sinus abnormalities; (2) 24 subjects (five male and 19 female) 16–70 years old (mean, 36 years) with pituitary adenomas, 23 of which were endocrine-secreting (Table 1), that were proved at surgery to infiltrate or invade the cavernous sinus; and (3) 25 subjects (nine male and 16 female) 17–81 years old (mean, 43 years) with pituitary adenomas, 11 of which were nonsecreting, that did not invade the cavernous sinus at surgery.

A retrospective analysis of images was performed by two observers. The coronal plane was the most useful for the assessment of the cavernous sinuses since it provides the clearest cross section of the pituitary, cavernous sinus, and dural reflections. Several qualitative and quantitative criteria were used to assess the cavernous sinus in all three groups: (1) the cavernous sinus was divided into medial, superior, lateral, and inferior compartments, and a linear measurement of each compartment was obtained (Fig. 1 and Table 2); (2) the distance between the medial walls of the horizontal intracavernous portion of the internal carotid arteries (intercarotid distance) was measured (Table 2); and (3) the visibility of the medial and lateral dural walls of the cavernous sinus was assessed.

Scans were evaluated for cavernous sinus involvement and divided into three groups: (1) no invasion, (2) definite invasion, and (3) questionable invasion. Several features were analyzed: the visibility of the medial dural reflection of the cavernous sinus; alterations in the size and intensity of the cavernous sinus compartments; and displacement or deformity of normal anatomic structures, including the presence and degree of carotid displacement and encasement. The criteria for carotid encasement included narrowing of vessel lumen and enveloping of the artery by tumor.

Prospective Analysis

After rereview of the retrospective group, the most reliable MR criteria suggesting CSI were applied prospectively in 30 patients with pituitary adenomas, and each scan was classified as either positive or negative for CSI and compared with the surgeon's operative assessment (Tables 3 and 4). The criteria emphasized were asymmetric signal intensity of the invaded cavernous sinus and the presence of carotid artery encasement. This group of 30 patients (16 females and 14 males) had 13 microadenomas (four prolactin-secreting, two growth hormone, and seven adrenocorticotropic hormone) and 17 macroadenomas (one growth-hormone, 11 nonsecreting, three prolactin-secreting, one adrenocorticotropic hormone, and one thyroid-stimulating hormone). The MR scans in this group were analyzed by two observers without prior knowledge of the surgical findings.

The MR examinations were performed on a 1.5-T unit. Imaging

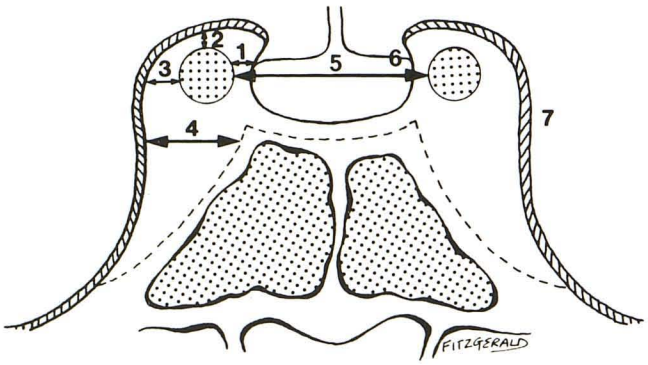

Fig. 1.—Coronal schematic of sellar and parasellar regions shows anatomic areas measured: medial (1), superior (2), lateral (3), and inferior (4) cavernous sinus compartments; distance between cavernous carotid arteries (5); and visibility of medial (6) and lateral (7) dural walls of cavernous sinus.

TABLE 1: Types of Secretory Activity in Pituitary Micro- and Macroadenomas with and Without Cavernous Sinus Invasion (Surgically Determined)

Tumor Type	No. of Adenomas					
	Cavernous Sinus Invasion			No Cavernous Sinus Invasion		
	Total	<10 mm	>10 mm	Total	<10 mm	>10 mm
Prolactin-secreting	14	8	6	5	4	1
Adrenocorticotropic hormone	6	4	2	1	1	0
Growth hormone	3	1	2	1	0	1
Thyroid-stimulating hormone	0	0	0	1	0	1
Mixed	0	0	0	6	4	2
Nonsecreting	1	0	1	11	1	10
Total	24	13	11	25	10	15

Note.—Microadenomas are <10 mm; macroadenomas are >10 mm.

TABLE 2: Measurements of Cavernous Sinus Compartments in Patients with and Without Pituitary Adenomas

Patient Group: Measurement	Mean Measurement in mm ± SEM (Significance[a])	
Normal:		
Medial compartment	1.14 ± 0.19	
Superior compartment	1.08 ± 0.11	
Lateral compartment	1.32 ± 0.14	
Inferior compartment	4.96 ± 0.26	
Intercarotid distance	16.60 ± 0.79	
	Adenomas < 10 mm	Adenomas >10 mm
Cavernous sinus invasion:		
Medial compartment	0.34 ± 0.20 ($p < .025$)	0.27 ± 0.19 ($p < .025$)
Superior compartment	1.26 ± 0.33 (NS)	3.81 ± 1.05 ($p < .0005$)
Lateral compartment	2.00 ± 0.43 (NS)	2.18 ± 0.87 (NS)
Inferior compartment	4.96 ± 0.62 (NS)	8.00 ± 1.27 ($p < .0005$)
Intercarotid distance	15.73 ± 0.86 (NS)	19.36 ± 0.96 ($p < .025$)
No cavernous sinus invasion:		
Medial compartment	0.95 ± 0.24 (NS)	0.40 ± 0.17 ($p < .01$)
Superior compartment	1.80 ± 0.35 (NS)	1.00 ± 0.17 (NS)
Lateral compartment	2.00 ± 0.47 (NS)	1.40 ± 0.15 (NS)
Inferior compartment	5.10 ± 0.48 (NS)	4.00 ± 0.28 (NS)
Intercarotid distance	16.60 ± 1.38 (NS)	20.46 ± 1.24 ($p < .005$)

Note.—NS = not significant.

[a] Significance was assessed relative to normal measurements.

TABLE 3: Analysis of MR Criteria for Cavernous Sinus Invasion Compared with Surgical Findings

Surgical Findings	Total	CS Asymmetry		Medial CS Wall Absent	Lateral CS Wall Bowed	Carotid Artery		Normal Gland Surrounding Tumor
		Size	Intensity			Displaced	Encased	
Retrospective:								
With cavernous sinus invasion:								
Microadenoma	13	0	2	13	0	0	1	NE
Macroadenoma	11	10	10	11	NE	6	3	NE
Subtotal	24	10	12	24	0	6	4	NE
Without cavernous sinus invasion:								
Microadenoma	10	0	0	7	NE	0	0	NE
Macroadenoma	15	1	1	15	NE	15	0	NE
Subtotal	25	1	1	22	NE	15	0	NE
Total	49	11	13	46	0	21	4	NE
Prospective:								
With cavernous sinus invasion:								
Microadenoma	5	3	3	5	0	0	2	0
Macroadenoma	4	2	2	4	0	0	1	0
Subtotal	9	5	5	9	0	0	3	0
Without cavernous sinus invasion:								
Microadenoma	8	0	2	5	2	0	0	1
Macroadenoma	13	1	1	13	2	6	0	1
Subtotal	21	1	3	18	4	6	0	2
Total	30	6	8	27	4	6	3	2

Note.—CS = cavernous sinus; NE = not evaluated.

parameters were 600/20/4 (TR/TE/excitations), 256 × 256 acquisition matrix, 16-cm field of view, and 3-mm sections (1-mm interslice gap). The acquisition time was 10–15 min and 23 sec for a standard T1-weighted imaging sequence. Both sagittal and coronal views were obtained. T2-weighted images were obtained in 32 of the 74 patients. Imaging parameters for T2-weighted sequences were 2000/40, 80/2, 128 × 256 acquisition matrix, 16-cm field of view, and 5-mm sections with 1-mm interslice gap.

TABLE 4: Retrospective and Prospective Correlation of MR Prediction of Cavernous Sinus Invasion with Surgical Results

Surgical Result	MR Prediction			% Sensitivity	% Specificity	% PPV	% NPV
	Positive	Negative	Equivocal				
Retrospective:							
Cavernous sinus invasion:							
Microadenoma	2	8	3				
Macroadenoma	10	0	1				
Total	12	8	4	60	NA	NA	NA
Prospective:							
Cavernous sinus invasion:							
Microadenoma	2	2	0				
Macroadenoma	3	2	0				
Subtotal	5	4	0				
No cavernous sinus invasion:							
Microadenoma	2	7	0				
Macroadenoma	1	11	0				
Subtotal	3	18	0				
Total	8	22	0	55	85.7	62.5	81.8

Note.—Sensitivity = true positive (TP)/[true positive + false negative (FN)]; specificity = true negative (TN)/[true negative + false positive (FP)]. PPV = positive predictive value (TP/(TP + FP) = fraction of patients with positive test results who have disease; NPV = negative predictive value (TN/(TN + FN) = fraction of patients with negative test results who are free of disease. NA = not attainable.

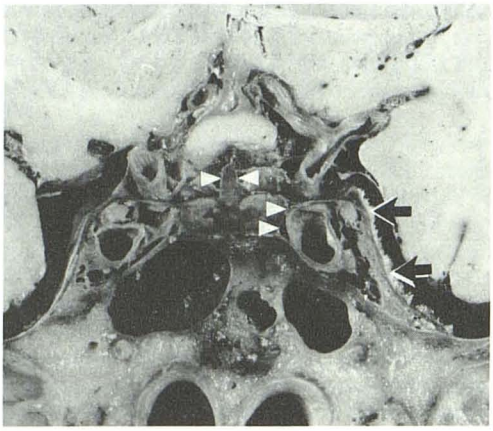

Fig. 2.—Coronal cadaver section of pituitary and pituitary stalk. Thin dural membrane demarcates medial margin of cavernous sinus (*arrowheads*), in contrast to thick lateral dural reflections (*arrows*). Stalk is midline.

Results

Retrospective Review

Normal cavernous sinus anatomy.—The cavernous sinus and sella could be seen on three to four contiguous 3-mm-thick sections, from the posterior to the anterior clinoids (Fig. 2). The normal cavernous sinuses were grossly symmetric, although their size and shape could show some minor variability (Fig. 3).

The cavernous sinus contents were primarily isointense relative to brain and interspersed with small foci of increased signal intensity representing fat or slow-flowing blood or both within the cavernous sinus (Fig. 3). The intracavernous carotid artery was readily identified by its characteristic thin walls surrounding a lumen of low signal intensity, reflecting high-velocity flow void (Fig. 3).

The position of the carotid artery within the cavernous sinus and its relationship to the pituitary were variable. The carotid siphon may be directly juxtaposed to the lateral margin of the pituitary gland (Fig. 3C), or it may be as far as 5 mm from the pituitary gland (Fig. 3B). The mean distance between the medial walls of the intracavernous portions of the siphon was 16.6 ± 0.79 mm (range, 10–24 mm) (Table 2).

The measurements of the various compartments of the cavernous sinus in each group are detailed in Table 2. Analysis of midpituitary coronal sections revealed that the normal mean medial cavernous sinus compartment measured 1.14 ± 0.19 mm (normal range, 0–5 mm) (Fig. 1). In fact, the medial cavernous sinus compartment was too small to be detected in 22 (44%) of the 50 normal cavernous sinuses examined, and was 5 mm wide in only one patient. The superior cavernous sinus compartment was 0–4 mm in size (Fig. 1). However, in nine (18%) of the 50 normal cavernous sinuses, the superior compartment was too small to be measured. The lateral compartment of the cavernous sinus also was quite small in the majority of patients, with a mean size of 1.32 ± 0.14 mm. In six (12%) of the 50 sinuses, it was 0 mm (Fig. 1). The inferior compartment of the cavernous sinus was 1–10 mm (mean, 4.96 ± 0.26 mm).

The lateral dural margin of the cavernous sinus was clearly visible on T1-weighted images as a linear structure of low signal intensity in 48 of 50 patients (Figs. 1–3). In two patients the lateral dural reflection was isointense on T1-weighted images, and, therefore, it was seen only on T2-weighted images. It was 0.5 mm thick and extended from the posterior to the anterior clinoids. The most medial part of the superior

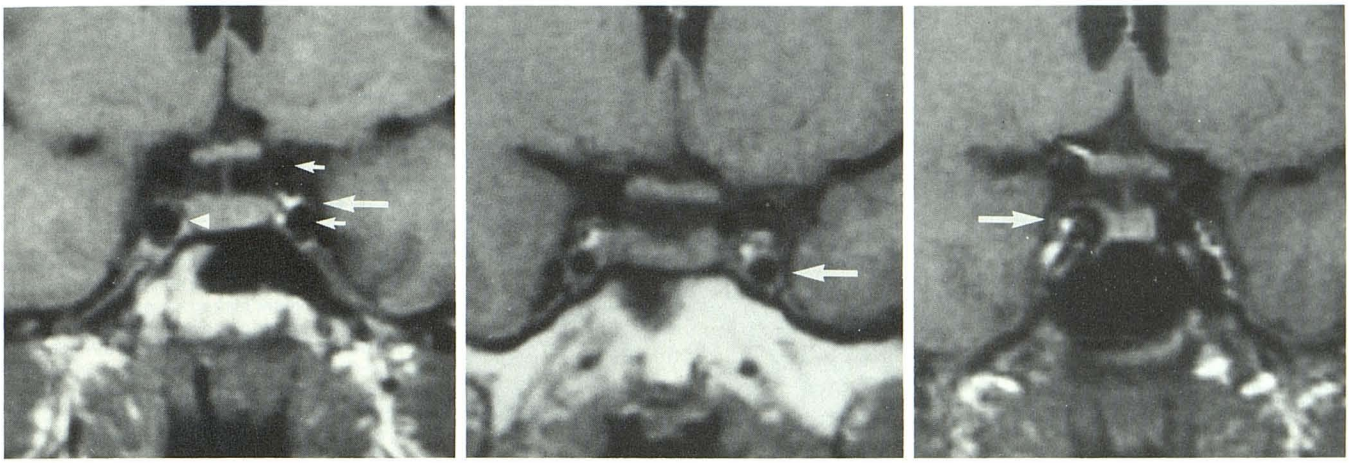

Fig. 3.—Normal anatomic variations of cavernous sinus in three subjects.

***A*, One of two patients in whom medial dural reflection separating pituitary from medial compartment of cavernous sinus is seen as thin, low-intensity line (*arrowhead*) (600/20 image). Portions of cavernous sinus are hyperintense owing to fat or slow-flowing venous blood. Intracavernous and supraclinoid carotid arteries appear as areas of signal void (*short arrows*). Medial cavernous sinus compartment measures 1 mm in transverse dimension. No lateral compartment can be identified. Lateral dural margin (*long arrow*).**

***B*, Prominent medial and superior cavernous sinus compartments. Medial dural reflection cannot be identified. Lateral dural margin (*arrow*).**

***C*, Intracavernous carotid arteries are very close to midline, there is no medial cavernous sinus compartment, and pituitary gland is indented by carotid artery on right. Lateral dural reflection of cavernous sinus is discrete hypointense line (*arrow*).**

Fig. 4.—31-year-old woman with recurrent 3-mm adrenocorticotropic hormone-secreting microadenoma on left side (*arrowheads*). At surgery, tumor infiltrated wall of cavernous sinus, producing asymmetric signal within left cavernous sinus (*curved arrow*) compared with normal right side (*straight arrow*).

Fig. 5.—25-year-old woman with 4-mm prolactinoma. Coronal T1-weighted image, 600/20, shows 4-mm low-density adenoma (*arrowheads*). Rim of higher intensity surrounds medial and inferior aspect of tumor and may represent compressed normal pituitary gland (*arrows*). However, hyperintense rim is incomplete on lateral aspect of tumor. No compromise is detected in medial compartment of cavernous sinus or asymmetric signal intensity of cavernous sinus. Pituitary stalk is midline in position. At surgery, tumor had penetrated anterior lobe on right side and had infiltrated dura of cavernous sinus at its junction with sellar floor.

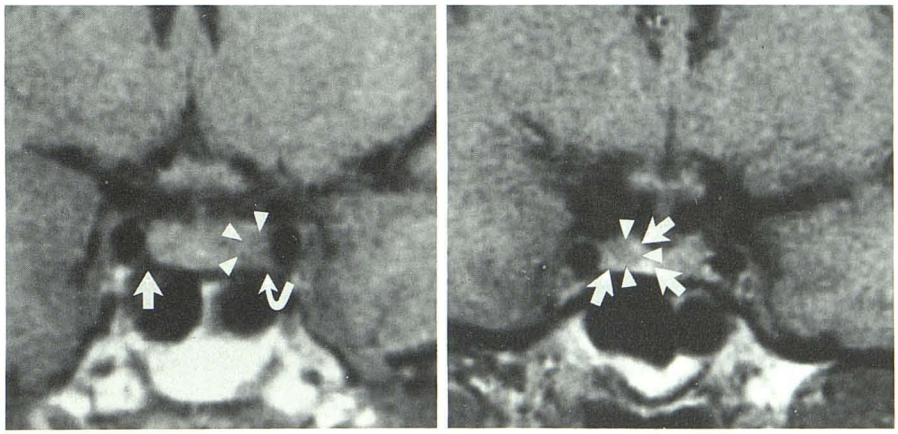

margin is the diaphragma sellae. It extends inferolaterally to the floor of the middle fossa (Figs. 1 and 3).

The medial dural reflection of the cavernous sinus, which separates the pituitary gland from the cavernous sinus and intracavernous carotid, was clearly seen on T1-weighted images as a thin, hypointense linear structure in only four of 50 normal sinuses (Fig. 3A).

Pituitary adenomas with and without CSI.—Surgical exploration revealed unilateral CSI in 24 patients and intact cavernous sinuses (by surgical inspection) in 25 patients (Tables 1 and 3). The cavernous sinuses were symmetric in size in all 13 invasive microadenomas and 10 noninvasive microadenomas. Although the mean size of the medial compartments of the cavernous sinuses was smaller in the invasive microadenomas than in the noninvasive microadenomas (Table 2), this was not a helpful differentiating feature in individual cases owing to the variability of this measurement in normal patients (Fig. 3C and Table 2).

Asymmetric cavernous sinus signal intensity was detected in only two of the 13 invasive microadenomas. Both were recurrent tumors, and the pathologic tissue, although small, produced an asymmetric signal compared with the contralateral cavernous sinus (Fig. 4). The cavernous sinuses were normal in most of the invasive microadenomas (Fig. 5). The cavernous sinuses were asymmetric in size and signal intensity in 10 of 11 invasive macroadenomas (Fig. 6), a feature seen in only one of the 15 noninvasive macroadenomas. In one patient, CSI was not detected on MR, even in retrospect (Fig. 7).

The medial wall of the cavernous sinus usually was not

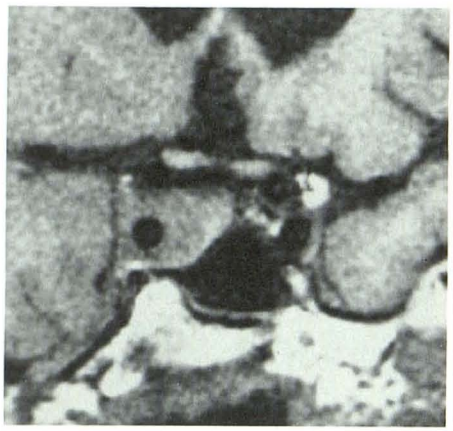

6

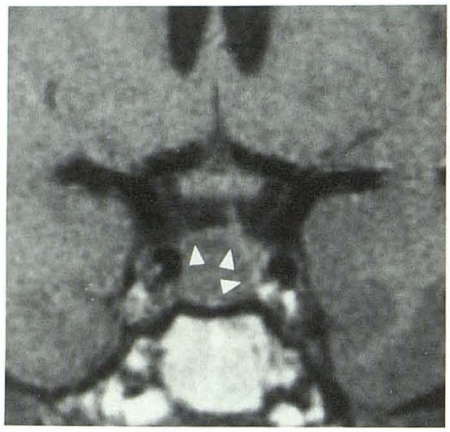

7

Fig. 6.—57-year-old man with invasive prolactinoma measuring more than 13 mm. There is definite asymmetric growth. Tumor extends into right cavernous sinus encasing right cavernous carotid artery. In comparison with opposite side, medial superior and lateral compartments are enlarged, and there is relative straightening of lateral dural reflection. At surgery, tumor was found to broadly invade right cavernous sinus, involving entire lateral wall of sella.

Fig. 7.—27-year-old woman with right-sided intrasellar macroadenoma. Displaced pituitary gland is of slightly higher intensity than tumor and can only be seen above and to left of lesion (*arrowheads*). Medial compartment of right cavernous sinus appears compressed; however, tumor does not encase or displace carotid artery. Medial dural reflection cannot be identified. At surgery, a tag of tissue was found to have invaded dura and entered right cavernous sinus.

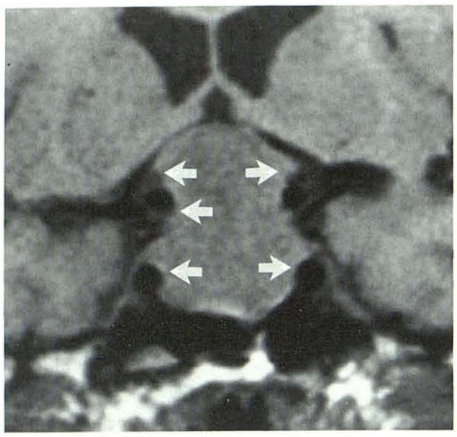

8

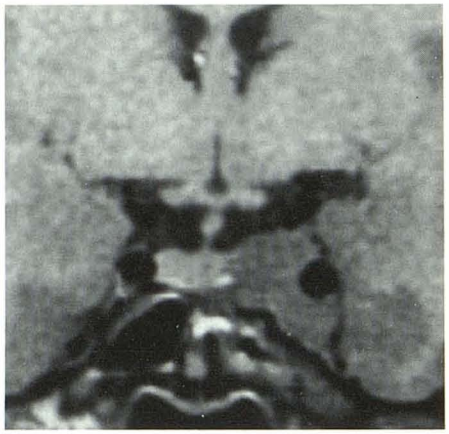

9

Fig. 8.—81-year-old woman with 35-mm nonsecreting, noninvasive macroadenoma. At surgery, tumor was completely excised and there was no evidence of infiltration of dura or invasion of cavernous sinus. Coronal T1-weighted image, 600/20, shows expansion of sella with 18 mm of suprasellar extension and secondary compression and stretching of optic chiasm. Thin rim of normal pituitary gland surrounds margin of tumor (*arrows*). Medial cavernous sinus compartments on both sides are compressed by tumor. Superior compartment is occupied by tumor as well. On the basis of the MR scan, it is not possible to determine whether tumor in medial and superior compartments resulted from displacement of medial dural reflection or invasion of medial dural reflection. In this case, clues to lack of cavernous sinus invasion are symmetric displacement of carotid arteries and apparent peripheral rim of compressed pituitary surrounding tumor. There is no convex bowing of lateral dural reflection of cavernous sinus.

Fig. 9.—14-mm nonsecreting recurrent pituitary adenoma, with surgically proved invasion of left cavernous sinus. Left carotid artery is surrounded by tumor and there is lateral bowing of lateral dural reflection as well as marked enlargement of medial and superior compartments by this tumor, which has signal intensity significantly lower than that of adjacent pituitary and temporal lobe.

seen in any of the three groups and, therefore, proved to be of little value in predicting CSI. Likewise, the lateral bowing of the dural margin of the cavernous sinus occurred in both patients with and without CSI.

Displacement of the cavernous segment of the carotid artery (widening of the intercarotid distance) occurred only with invasive (six of 11) and noninvasive (15 of 15) macroadenomas. However, in all 15 noninvasive macroadenomas, the carotid siphon was displaced bilaterally and associated with symmetric compression of the medial cavernous sinus compartment (Table 2 and Fig. 8), while in macroadenomas with CSI unilateral involvement of the cavernous sinus and occasional carotid encasement was the rule (Figs. 6 and 9). Encasement of the cavernous carotid artery (narrowing of the cross-sectional lumen) was uncommon (four of 24 tumors), and was present only with invasive tumors (Fig. 6 and Table 3).

The retrospective prediction of CSI by MR is shown in Table 4. MR suspected CSI in only two of the 13 patients with invasive microadenomas. MR was equivocal in four patients, while in another eight patients with surgical proof of CSI, it was not possible even in retrospect to determine the presence of CSI (Fig. 5). Excluding equivocal scans, CSI was suspected on MR scans in 12 of 20 patients with CSI at surgery (60% sensitivity).

Prospective Review

Thirty patients with pituitary tumor were studied prospectively for CSI by coronal and sagittal T1-weighted images

prior to surgery. The criteria evaluated in the retrospective limb were applied prospectively, and an overall assessment of the presence of CSI was made preoperatively on the basis of the most reliable criteria developed from the retrospective review (Tables 3 and 4). Of the 30 tumors, nine (five microadenomas and four macroadenomas) invaded the cavernous sinus at surgery while 21 (eight microadenomas and 13 macroadenomas) did not invade the cavernous sinus. The cavernous sinuses were asymmetrically increased in size and signal intensity in five (three microadenomas and two macroadenomas) of the nine patients with surgically proved CSI and in three of the 21 without CSI, corresponding to a sensitivity of 55% and a specificity of 85.7% for this one criterion (Table 3). The medial wall of the cavernous sinus could not be imaged in any of the nine patients with CSI and was seen in only three of the 21 patients without CSI. Thus, just as in the retrospective analysis, absence of the medial wall of the cavernous sinus is a poor predictor of CSI.

Bilateral displacement of the carotid arteries was present in six of the 13 noninvasive macroadenomas but in none of the macroadenomas with CSI. This finding agreed with the retrospective analysis in which all 15 tumors without CSI bilaterally displaced the carotid siphon. Thus, in this series of tumors, bilateral displacement of the carotid arteries occurred only with noninvasive, nonsecreting macroadenomas and was not associated with CSI.

Encasement of the carotid artery by pituitary adenoma was present in three of the nine invasive tumors (two microadenomas and one macroadenoma), but in none of the noninvasive tumors. Thus, when present, encasement of the carotid artery was the most specific sign indicating CSI.

Lateral bowing of the lateral cavernous sinus wall was not a sensitive indicator of CSI, as it was present in only four patients, all of whom had noninvasive tumors. Finally, in two patients with CSI (one microadenoma and one macroadenoma), a rim of compressed, normal pituitary gland, which was of higher intensity than tumor, separated the tumor from the cavernous sinus dura. This "rim" sign was helpful in excluding CSI only when the pituitary tissue was interposed between the tumor and cavernous sinus but did not exclude CSI when normal tissue was compressed medially by the tumor (Figs. 5, 7, and 8).

The prospective classification of the 30 MR scans into invasive and noninvasive groups was based on the most reliable criteria found from the retrospective review, namely, the presence of unilateral cavernous sinus enlargement and signal-intensity changes or the presence of carotid artery encasement. When either of these findings was present, the MR scans were classified as positive for CSI (Table 4). Comparison with the surgical findings revealed that MR agreed with the surgeon's impression in 23 of the 30 patients (Table 4). There were four false-negative MR scans and three false-positive MR scans (two microadenomas and one macroadenoma). The false-positive scans were interpreted as CSI on the basis of asymmetric signal intensity of the cavernous sinus adjacent to the tumor. The sensitivity of MR for predicting CSI in this prospective study was 55%, its specificity was 85.7%, its positive predictive value (a percentage of patients with a positive MR result who actually had cavernous sinus invasion) was 62.5%, and its negative predictive value (the percentage of patients with a negative MR who were actually without cavernous sinus invasion) was 81.8%. This correlates well with the retrospective analysis, in which MR had a sensitivity of 60% for the detection of CSI.

Discussion

In order to address the issue of detectability of CSI, an understanding of the normal cavernous sinus anatomy is paramount [17–30].

The cavernous sinus is lateral to the sphenoid bone, increasing in width in the axial plane from anterior to posterior. Dural reflections cover the lateral wall, superior wall, and base, as well as the most cephalad portion of the medial wall (Fig. 1). The thick lateral dura, which contains cranial nerves III–V, was identified by MR in almost all of our cases. The medial dura, which forms the pituitary capsule, is by contrast extremely thin. Thus far, neither MR nor CT have been able to reliably demonstrate the pituitary capsule. In fact, in the 50 normal cavernous sinuses reviewed, the medial dural reflection was identified in only four instances (two patients) on T1-weighted images and in none of the eight patients imaged with T2-weighted sequences.

Several reports have suggested that cavernous sinus involvement is more common than expected [1, 3–5, 7, 8]. Recent pathologic literature has supported the notion that microadenomas frequently invade the dura [2, 6]. Infiltration of the medial cavernous sinus dura may occur through venous sinusoids that drain from the pituitary gland into the cavernous sinus [1]. Since the size of the cavernous sinus is so variable, and since the medial dural reflection (pituitary capsule) cannot be identified on MR, it is unlikely that early infiltration of the dura can be identified on MR, or that invasion of the medial cavernous sinus can be distinguished from simple displacement of the medial cavernous sinus (Figs. 5 and 7). Owing to the above imaging limitations, dural infiltration by pituitary microadenoma, a common pathologic occurrence, cannot be identified reliably by MR. Advanced CSI usually can be identified on the basis of distortion of normal anatomy and an asymmetric increase in the size and intensity of the compartments of the cavernous sinus. In our retrospective review of patients with invasive adenomas, the most sensitive sign of CSI was an asymmetry in signal intensity between the two sides. However, the observation of slight asymmetric signal alterations in the cavernous sinus was responsible for the three false-positive MR readings in the prospective analysis and demonstrates the difficulty of making an accurate MR diagnosis on the basis of asymmetry of the cavernous sinus. The most specific sign of CSI was carotid artery encasement, which, although not often present, was seen only in those patients with CSI (Table 3). This was also found in our prospective analysis, in which encasement of the cavernous carotid artery, while only present in three of nine patients with CSI, was never seen with noninvasive tumors.

An interesting finding in our analysis was that CSI is exclusively unilateral. This may be a consequence of the fact that

the majority of invading tumors are prolactinomas, which originate from the lateral wing of the pituitary and thus more easily infiltrate the intervening normal pituitary gland to reach the pituitary capsule. In our retrospective group, the noninvasive macroadenomas were primarily nonsecreting tumors. Nonsecreting tumors tend to originate in the central portion of the pituitary, and are thus more likely to displace and compress the normal pituitary gland, preserving a thin peripheral rim of normal gland between tumor and the cavernous sinus that may prevent early dural infiltration (Fig. 8). However, this rim sign of noninvasive tumors was present in only two of the 21 noninvasive tumors prospectively evaluated, and therefore is of limited value. In addition, a rim of compressed gland may be present on the medial aspect of an invasive tumor (Fig. 7).

Displacement of the cavernous sinus without accompanying invasion is characterized by lateral displacement of the carotid siphon and compression of the medial compartment of the cavernous sinus with no enlargement of the superior, lateral, and inferior compartments. Bilateral, symmetric carotid displacement occurred only in macroadenomas without CSI; thus, when it was present it was a reliable sign excluding CSI (Fig. 8). However, a bias in this study may have been introduced by the fact that the reference or "gold standard" was not postmortem material, but rather the surgeon's impression during a transphenoidal resection. With macroadenomas, the surgeon cannot always identify the lateral extent of the tumor, and, therefore, his ability to assess expansion vs invasion at times may be limited. In our study, only cases in which the surgeon was able to directly visualize the cavernous sinus were included, thus reducing this bias.

It is of value to speculate on the comparative utility of CT. In our inspection of CT images in several of our patients, the medial dural reflection (pituitary capsule) could not be identified. The carotid arteries were not identified as readily as on MR, nor was the lateral dural reflection seen as clearly. Because both the cavernous sinus and pituitary adenomas enhance, it is unlikely that contrast-enhanced CT would improve sensitivity. There is a possibility that, as the intravascular pool diminishes, the enhancing pituitary tumor may be distinguished from the cavernous sinus blood pool. But again, this would not serve to distinguish between compression or invasion of the cavernous sinus.

In summary, although MR has proved to be the best technique for pituitary imaging, its sensitivity for CSI is only 55%. Unilateral carotid encasement within the cavernous sinus adjacent to a pituitary tumor is an infrequent but specific sign predicting CSI, while the presence of normal compressed pituitary interposed between the tumor and cavernous sinus (rim sign) or bilateral displacement of the carotid arteries by macroadenomas is more helpful in excluding CSI. While most invasive microadenomas do not alter the size or intensity of the cavernous sinus, the presence of asymmetric signal intensity or enlargement of the cavernous sinus adjacent to a pituitary tumor does not necessarily indicate CSI.

ACKNOWLEDGMENT

We thank Yolanda Eldred for assistance in manuscript preparation.

REFERENCES

1. Shaffi OM, Wrightson P. Dural invasion by pituitary tumors. *NZ Med J* **1975**;81:386–390
2. Selman WR, Laws ER, Scheithauer BW, Carpenter SM. *J Neurosurg* **1986**;64:402–407
3. Tumble HC. Pituitary tumours. *Br J Surg* **1951**;39:7–24
4. Martins AN, Hayes GJ, Kempe LG. Invasive pituitary adenomas. *J Neurosurg* **1965**;22:268–276
5. Lundberg PO, Drettner B, Hemmingsson A, Stenkvist B, Wide L. The invasive pituitary adenoma. *Arch Neurol* **1977**;34:742–749
6. Scheithauer BW, Kovacs KT, Laws ER, Randall RV. Pathology of invasive pituitary tumors. *J Neurosurg* **1986**;65:733–744
7. Landolt AM. Biology of pituitary microadenomas. In: Faglia G, Giovanelli MA, MacLeod RM, eds. *Pituitary microadenomas*. London: Academic, **1980**:107–122
8. Scheithauer BW. Surgical pathology of the pituitary and sellar region. In: Laws ER, Randall RV, Kesn EB, et al., eds. *Management of pituitary adenomas and related lesions*. New York: Appleton-Century-Crofts, **1986**:128–218
9. Wilson CB. A decade of pituitary microsurgery. *J Neurosurg* **1984**;61:814–833
10. Kline LB, Acker JD, Donovan-Post J, Vitek JJ. The cavernous sinus. *AJNR* **1981**;2299–2305
11. Hasso AN, Pop PM, Thompson JR, et al. High resolution thin section CT of the cavernous sinus. *RadioGraphics* **1982**;2(1):83–100
12. Ahmadi J, North CM, Segall HD, Zee CS, Weiss MH. Cavernous sinus invasion by pituitary adenomas. *AJNR* **1986**;6:893–898
13. Mark L, Pech P, Daniels D, Charles C, Williams A, Haughton V. The pituitary fossa: a correlative anatomic and MR study. *Radiology* **1984**;153:453–457
14. Bilaniuk LT, Zimmerman RA, et al. Magnetic resonance imaging of pituitary lesions using 1.0 to 1.5 T field strength. *Radiology* **1984**;153:415–418
15. Wiener SN, Rzeszotarski MS, Droege RT, Pearistein AE, Shafron M. Measurement of pituitary gland height with MRI. *AJNR* **1985**;6:717–722
16. Daniels DL, Pech P, Mark L, Pojunas K, Williams AL, Haughton VM. MRI of the cavernous sinus. *AJNR* **1985**;144:1009–1014
17. Taptas JN. Loge du sinus caverneux et sinus caverneux. *Sem Hop Paris* **1960**;36:1853–1860
18. Bedford MA. The cavernous sinus. *Br J Ophthalmol* **1966**;50:41–46
19. McGrath P. The cavernous sinus: an anatomical survey. *Aust NZ J Surg* **1977**;47:601–613
20. Patouillard P, Vanneurville G. Les parois du sinus caverneux. *Neurochirurgie* **1972**;10:551–560
21. Taptas JN. The so-called cavernous sinus. *Neurosurgery* **1982**;11(5):712–717
22. Harris FS, Rhoton AL. Anatomy of the cavernous sinus. *J Neurosurg* **1976**;45:169–180
23. Rajendran K, Ling EA. Light and scanning electron microscopical study of the cavernous sinus of the monkey. *J Anat* **1985**;140:229–235
24. Kaplan HA, Browder J, Krieger AJ. Intercavernous connections of the cavernous sinuses. *J Neurosurg* **1976**;45:166–168
25. Guidicelli G, Resche F, Louis R, Salamon G. Radioanatomie du sinus caverneux. *Neurochirurgie* **1972**;18:599–612
26. Theron J. Les affluents du plexus caverneux. *Neurochirurgie* **1972**;18:623–638
27. Vignaud J, Doyon D, Aubin ML, Clay C. Opacification du sinus caverneux par voix posterieure. *Neurochirurgie* **1972**;18:649–664
28. Bonnet P. La loge caverneuse et les syndormes de la loge caverneuse. *Arch Ophthalmol* **1955**;15(4):358–372
29. Butler H. Development of certain human dural venous sinuses. *J Anat* **1957**;91:510–526
30. Green HT. Venous drainage of the human hypophysis cerebri. *Am J Anat* **1957**;120:935–969